Bulletin of the Seismological Society of America, Vol. 93, No. 1, pp. 314–331, February 2003

Updated Near-Source Ground-Motion (Attenuation) Relations for the Horizontal and Vertical Components of Peak Ground Acceleration and Acceleration Response Spectra

by Kenneth W. Campbell and Yousef Bozorgnia

Abstract In this study we used strong-motion data recorded from 1957 to 1995 to derive a mutually consistent set of near-source horizontal and vertical ground-motion (attenuation) relations for peak ground acceleration and 5%-damped pseudo-acceleration response spectra. The database consisted of up to 960 uncorrected accelerograms from 49 earthquakes and 443 processed accelerograms from 36 earthquakes of M_W 4.7–7.7. All of the events were from seismically and tectonically active, shallow crustal regions located throughout the world. Some major findings of the study are (1) reverse- and thrust-faulting events have systematically higher amplitudes at short periods, consistent with their higher dynamic stress drop; (2) very firm soil and soft rock sites have similar amplitudes, distinctively different from amplitudes on firm soil and firm rock sites; (3) the greatest differences in horizontal ground motion among the four site categories occur at long periods on firm rock sites, which have significantly lower amplitudes due to an absence of sediment amplification, and at short periods on firm soil sites, which have relatively low amplitudes at large magnitudes and short distances due to nonlinear site effects; (4) vertical ground motion exhibits similar behavior to horizontal motion for firm rock sites at long periods but has relatively higher short-period amplitudes at short distances on firm soil sites due to a lack of nonlinear site effects, less anelastic attenuation, and phase conversions within the upper sediments. We used a relationship similar to that of Abrahamson and Silva (1997) to model hanging-wall effects but found these effects to be important only for the firmer site categories. The ground-motion relations do not include recordings from the 1999 $M_W > 7$ earthquakes in Taiwan and Turkey because there is still no consensus among strong-motion seismologists as to why these events had such low ground motion. If these near-source amplitudes are later found to be atypical, their inclusion could lead to unconservative engineering estimates of ground motion. The study is intended to be a limited update of the ground-motion relations previously developed by us in 1994 and 1997, with the explicit purpose of providing engineers and seismologists with a mutually consistent set of near-source ground-motion relations to use in seismic hazard studies. The U.S. Geological Survey and the California Geological Survey have selected the updated relation as one of several that they are using in their 2002 revision of the U.S. and California seismic hazard maps. Being a limited update, the study does not explicitly address such topics as peak ground velocity, sediment depth, rupture directivity effects, or the use of the 30-m velocity or related National Earthquake Hazard Reduction Program site classes. These are topics of ongoing research and will be addressed in a future update.

Introduction

In 1994, we developed a comprehensive near-source ground-motion (attenuation) relation for horizontal peak ground acceleration (PGA) in response to the 1992 Petrolia and Landers, California, earthquakes (Campbell and Bozorgnia, 1994). Campbell (1997) merged this 1994 relation with previous ground-motion relations that he had developed

for peak ground velocity (PGV), pseudoacceleration response spectra (PSA), and the vertical component of ground motion to use in engineering analysis (see Campbell, [1997] for a list of these previous relations). Many of these relations had different functional forms that led to a somewhat awkward and complicated set of ground-motion relations. In order to remedy this situation, we have repeated our 1994 analysis using a consistent set of strong-motion recordings and functional forms to develop a mutually consistent set of near-source ground-motion relations for the horizontal and vertical components of PGA and 5%-damped PSA. We also took this opportunity to update our PGA database with selected recordings from the 1994 Northridge, California, and 1995 Kobe (Hyogoken-Nanbu), Japan, earthquakes and to update our PSA database with these recordings plus selected recordings from earthquakes since 1987. Another important aspect of the study was to gain a better understanding of the characteristics of the vertical-to-horizontal response spectral ratio. This latter aspect of the study is the subject of another article (Bozorgnia and Campbell, 2002). A more detailed description of our study can be found in Bozorgnia *et al.* (1999) and Campbell and Bozorgnia (2000a,b).

It is important to recognize that this study was intended to be a limited update of the ground-motion relations developed by Campbell (1997), with the explicit purpose of providing engineers and seismologists with a mutually consistent set of near-source ground-motion relations for use in seismic hazard analysis. The U.S. Geological Survey (USGS) and the California Geological Survey (CGS) have selected these updated relations as one of several that they are using in their 2002 revision of the U.S. and California seismic hazard maps (Frankel *et al.*, 2002). As a limited update, the study does not explicitly address such topics as PGV, sediment depth, rupture directivity effects, or the use of the 30-m velocity or related National Earthquake Hazard Reduction Program (NEHRP) site classes. These topics are the subject of ongoing research and will be addressed at a later date. The study does, however, refine some of the parameters previously used by Campbell and Bozorgnia (1994) and Campbell (1997) by including hanging-wall effects, by dividing their reverse-faulting events into reverse- and thrust-faulting categories, and by dividing their generic soil sites into firm and very firm soil categories. We retained the use of the soft rock and hard rock categories in these studies, though we renamed the latter "firm rock" to avoid confusion with the much firmer hard rock sites in eastern North America.

Four important earthquakes occurred toward the end of our study that we decided not to include in this limited update. These were the 17 August 1999 Kocaeli (Izmit), Turkey, earthquake (M_W 7.4), the 21 September 1999 Chi-Chi, Taiwan, earthquake (M_W 7.6), the 16 October 1999 Hector Mine, California, earthquake (M_W 7.1), and the 12 November 1999 Duzce, Turkey, earthquake (M_W 7.1). These earthquakes, especially the Izmit and Chi-Chi events, are important because they provide near-source recordings at magnitudes for which the strong-motion database is extremely limited. However, a preliminary analysis of the ground motion from these two earthquakes indicates that their median short-period ground motion is significantly smaller than that predicted from contemporary ground-motion relations (see also Anderson, 2000; Youd *et al.*, 2000; Tsai *et al.*, 2000; Boore, 2001; Chang *et al.*, 2001; Akkar and Gulkan, 2002; Atakan *et al.*, 2002). There has been some speculation that this ground motion might be lower than expected because the causative faults had large total slip (Anderson *et al.*, 2000; Anderson, 2003) or that the events themselves had significant surface rupture (Somerville, 2000) or long dislocation rise time (Zeng and Chen, 2001). Including these recordings in our ground-motion relations would lower the predicted near-source ground motion, possibly significantly, because of the limited number of recordings at these magnitudes. It was our concern, plus the concern of Anderson *et al.* (2000) and other investigators we talked to (e.g., N. Abrahamson, personal comm., 2002; D. Boore, personal comm., 2002) that these recordings might not represent the average ground motion from earthquakes of similar magnitude. If this were the case, including them could lead to an underprediction of engineering estimates of ground motion from large earthquakes. Therefore, like many of our colleagues, we have chosen to wait to include the 1999 strong-motion data until we better understand the possible causes for their potentially low ground motion.

Strong-Motion Database

We used a comprehensive database of near-source worldwide accelerograms recorded over the 39-yr time period from 1957 to 1995 to derive our updated ground-motion relations. The database was expanded and updated from that originally used by Campbell and Bozorgnia (1994) and Campbell (1997). We expanded the database to include PGA values from two earthquakes that occurred from 1992 to 1995 and PSA values from 11 earthquakes that occurred from 1987 to 1995. In addition, we augmented the previous database with additional recordings that had become available since the original compilation (Table 1).

The strong-motion parameters included uncorrected peak ground acceleration (uncorrected PGA), corrected peak ground acceleration (corrected PGA), and 5%-damped PSA at natural periods ranging from 0.05 to 4 sec. The terms uncorrected and corrected refer to the standard levels of accelerogram processing commonly referred to as phases 1 and 2, respectively. Uncorrected PGA was either scaled directly from the recorded accelerogram or, if the accelerogram was processed, from the baseline- and instrument-corrected phase 1 acceleration time history. Corrected PGA was measured from the phase 2 acceleration time history after it had been bandpass filtered and decimated to a uniform time interval. Response spectral ordinates were taken directly from the processed phase 3 (response and Fourier spectra) data, if available, or calculated from the phase 2 processed accelerogram, if these data were not available. In all cases, we

Table 1
Database of Strong-Motion Recordings

Earthquake	Location	Year	M_W	Faulting Mechanism	No. of Recordings			
					Uncorrected		Corrected	
					Horizontal	Vertical	Horizontal	Vertical
Daly City	California	1957	5.3	Reverse oblique	1	1	1	1
Parkfield	California	1966	6.1	Strike slip	4	4	4	4
Koyna	India	1967	6.3	Strike slip	1	1	1	1
Lytle Creek	California	1970	5.3	Reverse	6	6	4	4
San Fernando	California	1971	6.6	Reverse	11	11	9	9
Sitka	Alaska	1972	7.7	Strike slip	1	1	1	1
Stone Canyon	California	1972	4.7	Strike slip	3	3	2	2
Managua	Nicaragua	1972	6.2	Strike slip	1	1	1	1
Point Mugu	California	1973	5.6	Reverse	1	1	0	0
Hollister	California	1974	5.1	Strike slip	1	1	1	1
Oroville	California	1975	6.0	Normal	4	4	1	1
Kalapana	Hawaii	1975	7.1	Thrust	1	1	0	0
Gazli	Uzbekistan	1976	6.8	Reverse	1	1	1	1
Caldiran	Turkey	1976	7.3	Strike slip	1	1	1	1
Mesa de Andrade	Mexico	1976	5.6	Strike slip	3	0	0	0
Santa Barbara	California	1978	6.0	Thrust	3	3	1	1
Tabas	Iran	1978	7.4	Thrust	3	3	3	3
Bishop	California	1978	5.8	Strike slip	3	3	0	0
Malibu	California	1979	5.0	Reverse	1	1	0	0
St. Elias	Alaska	1979	7.6	Thrust	1	0	1	0
Coyote Lake	California	1979	5.8	Strike slip	17	11	9	9
Imperial Valley	California	1979	6.5	Strike slip	43	43	37	37
Livermore	California	1980	5.8	Strike slip	9	9	0	0
Livermore Aftershock	California	1980	5.4	Strike slip	10	10	0	0
Westmorland	California	1981	6.0	Strike slip	23	23	0	0
Coalinga	California	1983	6.4	Thrust	50	50	46	46
Morgan Hill	California	1984	6.2	Strike slip	39	39	24	24
Nahanni	Canada	1985	6.8	Thrust	3	2	3	2
North Palm Springs	California	1986	6.1	Strike slip	40	40	12	12
Chalfant Valley	California	1986	6.3	Strike slip	13	13	0	0
Whittier Narrows	California	1987	6.0	Thrust	141	138	91	90
Whittier Narrows Aftershock	California	1987	5.3	Reverse oblique	44	44	9	9
Elmore Ranch	California	1987	6.2	Strike slip	25	25	1	1
Superstition Hills	California	1987	6.6	Strike slip	30	30	2	2
Spitak	Armenia	1988	6.8	Reverse oblique	1	0	1	0
Pasadena	California	1988	5.0	Strike slip	15	15	0	0
Loma Prieta	California	1989	6.9	Reverse oblique	51	50	29	29
Malibu	California	1989	5.0	Thrust	6	6	0	0
Manjil	Iran	1990	7.4	Strike slip	3	3	3	3
Upland	California	1990	5.6	Strike slip	41	41	2	2
Sierra Madre	California	1991	5.6	Reverse	69	68	4	4
Landers	California	1992	7.3	Strike slip	18	18	8	8
Big Bear	California	1992	6.5	Strike slip	22	22	1	1
Joshua Tree	California	1992	6.2	Strike slip	13	13	0	0
Petrolia	California	1992	7.0	Thrust	13	11	5	5
Petrolia Aftershock	California	1992	7.0	Strike slip	5	5	0	0
Erzincan	Turkey	1992	6.7	Strike slip	1	1	1	1
Northridge	California	1994	6.7	Thrust	149	149	108	108
Kobe	Japan	1995	6.9	Strike slip	15	15	15	15

used the geometric mean of the two horizontal components of PGA or PSA to define what we hereafter call the average horizontal component of ground motion.

The database of uncorrected PGA included 960 average horizontal components from 49 worldwide earthquakes and 941 vertical components from 46 worldwide earthquakes of moment magnitude (M_W) 4.7–7.7. This represents a 50% increase in the number of uncorrected recordings that were used in the previous analysis of uncorrected PGA by Campbell and Bozorgnia (1994) and Campbell (1997). The database of corrected PGA and PSA included 443 average horizontal components from 36 worldwide earthquakes and 439 vertical components from 34 worldwide earthquakes of M_W 4.7–7.7. This represents a 100% increase in the number of

horizontal recordings and a 150% increase in the number of vertical recordings that were used in the previous analysis of corrected PGA and PSA by Campbell (1997). It is important to note that the uncorrected database has over double the number of recordings than the corrected database. The importance of this difference on the regression results is discussed by Bozorgnia *et al.* (1999) and Campbell and Bozorgnia (2000a,b). The distribution of the recordings with respect to magnitude and distance is shown in Figure 1, and their distribution by faulting mechanism and local site conditions is given in Table 2. The shot-gun pattern exhibited in Figure 1, statistically referred to as homoscedasticity, suggests that there was no need to use special statistical procedures to decouple source and path effects in the regression analysis, at least over the M_W 6.0–7.5 magnitude range that is of greatest engineering interest.

Because our interest is in shallow crustal earthquakes in seismically and tectonically active regions, we included only earthquakes with focal depths less than 25 km located in seismic regions believed to have source and near-source attenuation characteristics similar to western North America. However, there is some controversy whether all of the selected earthquakes occurred in such an environment. For example, Atkinson and Boore (1998) included the 1976 Gazli and the 1985 Nahanni earthquakes in their list of events from stable continental regions. Since the seismological community has yet to come to a consensus on this issue, we included both of these earthquakes in our study. Unlike the previous studies of Campbell and Bozorgnia (1994) and Campbell (1997), we excluded subduction-interface earthquakes, since such events occur in an entirely different tectonic environment than the other shallow crustal earthquakes that were analyzed in our study, and it has not been clearly shown that their near-source ground motion is similar to that of shallow crustal earthquakes.

We uniformly defined the size of an earthquake in terms of M_W and defined the source-to-site distance in terms of r_{seis}, defined as the shortest distance between the recording site and the zone of the seismogenic energy release on the causative fault (referred to here as the distance to seismogenic rupture). We restricted recording sites to $r_{seis} \leq 60$ km to avoid complications related to the arrival of multiple reflections from the lower crust, as was observed during the 1989 Loma Prieta earthquake (Somerville and Yoshimura, 1990; Campbell, 1991, 1998). We believe that this distance range includes most ground-motion amplitudes of engineering interest. We defined sediment depth as the depth to firm rock (see definition for firm rock below), if this rock were relatively shallow, or, if this depth was not known, to the depth to rock having a shear-wave velocity of about 2.5 km/sec or greater or having a compressional-wave velocity of about 4.3 km/sec or greater. Sediment depth has been found in past studies to be strongly correlated with the amplitude of long-period spectral acceleration (Campbell, 1989, 1997; Trifunac and Lee, 1989, 1992; Field, 2000; Lee and Anderson, 2000). Joyner (2000) found that the amplification of

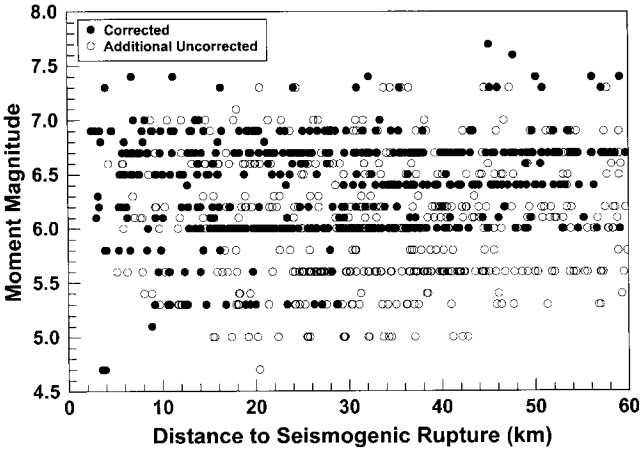

Figure 1. Distribution of recordings used in the regression analysis of peak ground acceleration and spectral acceleration (5%-damping). Solid circles represent recordings from the corrected database, and open circles represent additional recordings from the uncorrected database.

long-period ground motion predicted from sediment depth from the ground-motion relation of Campbell (1997) was reasonably consistent with the predicted amplification from surface-wave generation at the edge of the Los Angeles Basin. Field and the SCEC Phase III Working Group (2000) found that sediment depth was a reasonable proxy for representing the average three-dimensional response of the Los Angeles Basin calculated from a suite of hypothetical earthquakes occurring within and outside the basin (Olsen, 2000).

We classified the faulting mechanism of an earthquake into one of three categories defined as strike slip, reverse, or thrust. The strike-slip category includes earthquakes on vertical or near-vertical faults with rake angles (the orientation of slip on the fault) within $\pm 22.5°$ of the strike of the fault. The reverse and thrust categories include steeply and shallow ($\leq 45°$) dipping earthquakes, respectively, with rake angles between 22.5° and 157.5°. The thrust category includes blind thrust events such as the 1983 Coalinga, 1987 Whittier Narrows, and 1994 Northridge, California, earthquakes. The strike-slip category includes four recordings from the 1985 Oroville normal-faulting earthquake. Based on a comparison with the Boore *et al.* (1997) ground-motion relation, Spudich *et al.* (1999) concluded that earthquakes with normal-faulting mechanisms in extensional stress environments have lower median predicted ground motion at some periods and distances than earthquakes that occur in compressional stress environments. However, these authors also included strike-slip earthquakes from the Imperial Valley, California, in their extensional database, which were also included in our study and in many other empirical studies using western North American data. They also noted that by constraining their site parameter, they built in an inherent underprediction of their ground-motion estimates on rock, which might have contributed, at least partially, to their conclusion. Therefore,

Table 2
Distribution of Recordings by Faulting Mechanism and Local Site Conditions

Type of Faulting or Local Site Conditions	Uncorrected Database								Corrected Database							
	No. of Recordings		No. of Events		Min. Magnitude		Max. Magnitude		No. of Recordings		No. of Events		Min. Magnitude		Max. Magnitude	
	H	V	H	V	H	V	H	V	H	V	H	V	H	V	H	V
Faulting Mechanism																
Strike slip faulting	404	395	29	28	4.7	4.7	7.7	7.7	127	127	20	20	4.7	4.7	7.7	7.7
Reverse faulting	186	183	10	9	5.0	5.0	6.9	6.9	58	57	8	7	5.3	5.3	6.9	6.9
Thrust faulting	370	363	10	9	5.0	5.0	7.6	7.4	258	255	8	7	6.0	6.0	7.6	7.4
TOTAL	960	941	49	46	—	—	—	—	443	439	36	34	—	—	—	—
Local Site Conditions																
Firm soil	534	525	42	40	4.7	4.7	7.4	7.4	241	240	30	29	4.7	4.7	7.4	7.4
Very firm soil	168	166	23	23	4.7	4.7	7.0	7.0	84	83	14	14	4.7	4.7	7.0	7.0
Soft rock	126	124	20	19	5.0	5.0	7.6	6.9	63	62	9	8	5.3	5.3	7.6	6.9
Firm rock	132	126	32	31	5.0	5.0	7.7	7.7	55	54	21	21	5.3	5.3	7.7	7.7
TOTAL	960	941	—	—	—	—	—	—	443	439	—	—	—	—	—	—

consistent with past studies, we included a few earthquakes that Spudich *et al.* (1999) would claim come from an extensional stress environment in our strike-slip category. We define normal-faulting earthquakes as events with rake angles between 202.5° and 337.5°.

We classified local site conditions at each recording site into one of four categories defined as firm soil, very firm soil, soft rock, or firm rock. The firm soil category generally includes soil deposits of Holocene age (less than 11,000 years old), described principally on geologic maps as recent alluvium, alluvial fans, or undifferentiated Quaternary deposits. The very firm soil category generally includes soil deposits of Pleistocene age (11,000 to 1.5 million years old), described principally on geologic maps as older alluvium or terrace deposits. The soft rock category generally includes sedimentary rock and "soft," Tertiary volcanic deposits (1.5 to 100 million years old) as well as "softer" units of the Franciscan Complex and other low-grade metamorphic rocks generally described as melange, serpentine, and schist. The firm rock category generally includes pre-Tertiary sedimentary rock and "hard" volcanic deposits, high-grade metamorphic rock, crystalline rock, and the "harder" units of the Franciscan Complex generally described as sandstone, graywacke, shale, chert, and greenstone. These site categories are the same as the Holocene soil, Pleistocene soil, soft rock, and hard rock categories defined by Campbell and Bozorgnia (1994) and Campbell (1997). The names of the soil categories were changed to make them more descriptive of their implied stiffness rather than their geologic age. The name of the hard rock category was changed so that it would not be confused with the hard rock units of eastern North America.

The geologic-based site categories defined in this study can be approximately related to the average shear-wave velocity in the top 30 m of the site, V_{S30}, based on statistical analyses of measured V_{S30} for similar geologic units reported by Wills and Silva (1998) and Wills *et al.* (2000) for all of California and by Park and Elrick (1998) for southern California. These relationships are summarized in Table 3. Three observations are clear from this table: (1) there is considerable variability in the mean estimates of V_{S30} among the different compilations, although these differences are not necessarily statistically significant; (2) the standard deviation of an individual estimate of V_{S30} for a given site category varies anywhere from about 20% to 35% of its mean value; and (3) the mean value of V_{S30} for some studies and categories are based on a relatively small number of measurements. For the more robust Wills and Silva (1998) study, velocities are given for the two major geologic units of our firm rock category, namely, crystalline rock (located primarily in southern California) and Franciscan Complex (located primarily in northern California). A hypothesis test of the difference in the means of the Wills and Silva (1998) velocities for the different site categories listed in Table 3 indicated that the hypothesis that this difference is zero can be rejected at the 5% level of significance for all categories, except for the comparison between crystalline rock and Franciscan Complex. Therefore, we suggest that the means and standard deviations of V_{S30} given by Wills and Silva (1998) can be used as reasonable estimates of the velocities for the four site categories defined in our study. The velocity ranges that represent the mean $\pm$ standard deviation for our firm soil, very firm soil, soft rock, and firm rock site categories correspond approximately to NEHRP soil classes D, CD, CD, and BC defined by Wills *et al.* (2000).

All of the selected recordings come from free-field sites, which we defined as instrument shelters or nonembedded buildings less than three stories high (less than seven stories high if located on firm rock). We included recordings on dam abutments to enhance the database of rock recordings, even though there could be some interaction between the dam and the recording site. We excluded recordings in the basements of buildings of any size, in buildings over two stories high (over six stories high if located on firm rock),

Table 3
Relationship between Site Categories and Site Velocity

	Wills and Silva (1998)			Wills *et al.* (2000)			Park and Elrick (1998)		
Site Category	Units	V_{S30} (m/sec)*	No.	Units	V_{S30} (m/sec)	No.	Units	V_{S30} (m/sec)	No.
Firm soil	Qal	298 ± 92	237	D	301 ± 92	239	Qyc, Qym, Qyf	325 ± 59†	21
Very firm soil	Q. old alluvium	368 ± 80	79	CD	372 ± 98	154	Qoc, Qom, Qof	391 ± 22	11
Soft rock	Tertiary	421 ± 109	40	—	—	—	Tss	411 ± 79	5
Firm rock	Plutonic, Metamorphic, KJF	830 ± 339	47	BC	718 ± 355	45	—	—	—
Crystalline	Plutonic, metamorphic	715 ± 242	18	—	—	—	Mxb	781 ± 240	4
Franciscan	KJF	902 ± 387	29	—	—	—	—	—	—

*Mean plus and minus one standard deviation.
†Standard deviation has been calculated from standard deviation of the logarithm assuming a lognormal distribution.

or on the toe or base of a dam because of the potential adverse effects of instrument embedment and soil-structure interaction (Campbell, 1997). Stewart (2000) gives a more engineering-based empirical technique that can be used to identify spectral ordinates with significant soil–structure interaction effects that we hope to apply in a future update of our ground-motion relations.

Ground-Motion Relations

The equation we selected to represent the ground-motion relations for both the average horizontal and vertical components of PGA and PSA is given by

$$\ln Y = c_1 + f_1(M_W) + c_4 \ln \sqrt{f_2(M_W, r_{seis}, S)} + f_3(F) + f_4(S) + f_5(\mathrm{HW}, F, M_W, r_{seis}) + \varepsilon, \quad (1)$$

where the magnitude scaling characteristics are given by

$$f_1(M_W) = c_2 M_W + c_3(8.5 - M_W)^2, \quad (2)$$

the distance scaling characteristics are given by

$$f_2(M_W, r_{seis}, S) = r_{seis}^2 + g(S)^2 \left(\exp[c_8 M_W + c_9(8.5 - M_W)^2]\right)^2, \quad (3)$$

in which the near-source effect of local site conditions is given by

$$g(S) = c_5 + c_6(S_{VFS} + S_{SR}) + c_7 S_{FR}, \quad (4)$$

the effect of faulting mechanism is given by

$$f_3(F) = c_{10} F_{RV} + c_{11} F_{TH}, \quad (5)$$

the far-source effect of local site conditions is given by

$$f_4(S) = c_{12} S_{VFS} + c_{13} S_{SR} + c_{14} S_{FR}, \quad (6)$$

and the effect of the hanging wall (HW) is given by

$$f_5(\mathrm{HW}, F, M_W, r_{seis}) = \mathrm{HW} f_3(F) f_{HW}(M_W) f_{HW}(r_{seis}), \quad (7)$$

where

$$\mathrm{HW} = \begin{cases} S_{VFS} + S_{SR} & \text{for } r_{jb} \geq 5 \text{ km} \\ S_{FR} & \text{otherwise } \delta > 70^\circ, \end{cases} \quad (8)$$

$$f_{HW}(M_W) = \begin{cases} 0 & \text{for } M_W < 5.5 \\ M_W - 5.5 & \text{for } 5.5 \leq M_W \leq 6.5 \\ 1 & \text{for } M_W > 6.5, \end{cases} \quad (9)$$

and

$$f_{HW}(r_{seis}) = \begin{cases} c_{15}(r_{seis}/8) & \text{for } r_{seis} < 8 \text{ km} \\ c_{15} & \text{for } r_{seis} \geq 8 \text{ km}. \end{cases} \quad (10)$$

In the previous equations, Y is either the vertical component, Y_V, or the average horizontal component, Y_H, of PGA or 5%-damped PSA in g (g = 981 cm/sec^2); M_W is moment magnitude; r_{seis} is the closest distance to seismogenic rupture in kilometers; r_{jb} is the closest distance to the surface projection of fault rupture in kilometers (Boore *et al.*, 1997); δ is fault dip in degrees; S_{VFS} = 1 for very firm soil, S_{SR} = 1 for soft rock, S_{FR} = 1 for firm rock, and $S_{VFS} = S_{SR} = S_{FR} = 0$ for firm soil; F_{RV} = 1 for reverse faulting, F_{TH} = 1 for thrust faulting, and $F_{RV} = F_{TH} = 0$ for strike-slip and normal faulting; and ε is a random error term with zero mean and standard deviation equal to $\sigma_{\ln Y}$.

The standard deviation, $\sigma_{\ln Y}$, is defined either as a function of magnitude,

$$\sigma_{\ln Y} = \begin{cases} c_{16} - 0.07 M_W & \text{for } M_W < 7.4 \\ c_{16} - 0.518 & \text{for } M_W \geq 7.4, \end{cases} \quad (11)$$

or as a function of PGA,

$$\sigma_{\ln Y} = \begin{cases} c_{17} + 0.351 & \text{for PGA} \le 0.07g \\ c_{17} - 0.132\ln(\text{PGA}) & \text{for } 0.07g < \text{PGA} < 0.25g \\ c_{17} + 0.183 & \text{for PGA} \ge 0.25g, \end{cases} \quad (12)$$

where PGA is either uncorrected PGA or corrected PGA, depending on whether uncorrected PGA or whether corrected PGA and/or PSA is being predicted. The parameters c_1 through c_{17} are coefficients to be determined from the data.

The exponential magnitude term in equation (3) accounts for the magnitude dependence of Y with distance. Based on a preliminary analysis, we constrained the coefficients in this term in order to make Y independent of M_W at $r_{seis} = 0$ km, an attribute commonly referred to as magnitude saturation. Otherwise, Y exhibited oversaturation and was found to decrease with magnitude at close distances. The constraint was applied by setting $c_8 = -c_2/c_4$ and $c_9 = -c_3/c_4$ in equation (3). The regression coefficients c_5 through c_7 in equation (4) allow the value of Y for different site categories to vary with both distance and magnitude, thus permitting the possibility of nonlinear site effects and different near-source attenuation characteristics among soil categories. As discussed previously, we did not include sediment depth as a parameter in the regression analysis even though an analysis of residuals (discussed in a later section) indicated that it is an important parameter, at least at long periods. We do not believe that its exclusion is a serious practical limitation of the model because sediment depth is generally not used in engineering analyses, and it is not included in any other ground-motion relation widely used in seismology and engineering. Therefore, the results represent an average sediment depth. We will include this parameter in a future study once its correlation with other parameters is better understood.

The relationship for hanging-wall effects given in equations (7) through (10) is an adaptation of that given by Abrahamson and Silva (1997). An analysis of residuals indicated that this relationship could be used with our ground-motion relation with only a few modifications. First, we found that hanging-wall effects were important only for very firm soil, soft rock, and firm rock. Apparently, the nonlinear site effects inherent in large ground motion on firm soil do not permit a significant increase in ground motion over the hanging wall. Second, the hanging wall is defined as a 5-km margin around the surface projection of the rupture surface, which can be represented by the distance measure r_{jb} defined by Boore *et al.* (1997). Last, the hanging-wall effect dies out for $r_{seis} < 8$ km, or sooner if $r_{jb} \ge 5$ km or $\delta \ge 70°$.

We provide two alternative relationships for $\sigma_{\ln Y}$, consistent with our previous analyses. We prefer the one in terms of PGA because it is statistically more robust. The relationship in terms of M_W is included for consistency with other studies and for use by those who prefer such a relationship. As pointed out by Steve Harmsen (personal comm., 2002), there are very few recordings that can be used to constrain the value of $\sigma_{\ln Y}$ for large earthquakes. On the other hand, there are a large number of recordings that can be used to constrain the value of $\sigma_{\ln Y}$ for PGA $\ge 0.25g$.

We determined the coefficients c_1 through c_{17} from regression analysis, using the method of generalized nonlinear least squares. As in the previous analysis by Campbell and Bozorgnia (1994), we did not apply weights during the regression analysis because of the relatively uniform distribution of recordings with respect to magnitude and distance (Fig. 1). To make the regression analysis of corrected PGA and PSA more stable, c_2 (the magnitude coefficient) was set equal to the value determined from the better-constrained analysis of uncorrected PGA. Monte Carlo simulation indicated that all of the regression coefficients were statistically significant at the 10% level. As in any independent regression analysis on individual spectral ordinates, there was a considerable amount of period-to-period variability in the regression coefficients that led to variability in the predicted acceleration response spectra, especially when extrapolated to small distances and large magnitudes. In order to reduce this variability, we did a limited amount of smoothing of the regression coefficients. These smoothed coefficients are listed in Table 4. The resulting ground-motion relations for selected response spectral ordinates are plotted in Figure 2. Predicted response spectra showing the effects of magnitude, faulting mechanism, and local site conditions are plotted in Figure 3.

Figure 3 shows that the behavior of spectral acceleration with site conditions is significantly different between the horizontal and vertical spectra. For the horizontal component, the amplitudes for firm soil and firm rock are somewhat higher at short periods and the amplitudes for firm rock are significantly lower at long periods for the specific values of magnitude ($M_W = 7.0$) and distance ($r_{seis} = 10$ km) used in the evaluation. The short-period amplitudes for firm soil (not shown) are found to be much higher than the other site categories for smaller ground motions, consistent with reduced nonlinear site effects. For the vertical component, the amplitudes for firm soil are significantly higher at short periods and the amplitudes for firm rock are substantially lower at long periods. This is true for smaller ground motions as well. Very firm soil and soft rock have similar amplitudes at all periods for both the horizontal and vertical components.

Figure 3 also shows that both the horizontal and vertical spectra have the same tendency toward higher amplitudes for reverse and thrust faulting at short-to-mid periods. These differences become negligible at periods greater than about 2 sec. This trend is consistent with the expectation that reverse- and thrust-faulting earthquakes, especially from blind thrust faults, might have on average higher dynamic stress drops than strike-slip and normal-faulting earthquakes. Thrust-faulting events have somewhat higher amplitudes at some periods compared to reverse-faulting events, but this difference is generally less than about 10%. This small difference was unexpected considering the relatively large ground motion observed during the 1987 Whittier Narrows

Table 4

Coefficients and Statistical Parameters from the Regression Analysis of PGA and PSA

T_n (sec)	c_1	c_2	c_3	c_4	c_5	c_6	c_7	c_8	c_9	c_{10}	c_{11}	c_{12}	c_{13}	c_{14}	c_{15}	c_{16}	c_{17}	No.	r^2
Average Horizontal Component																			
Unc. PGA	−2.896	0.812	0.000	−1.318	0.187	−0.029	−0.064	0.616	0	0.179	0.307	−0.062	−0.195	−0.320	0.370	0.964	0.263	960	0.955
Cor. PGA	−4.033	0.812	0.036	−1.061	0.041	−0.005	−0.018	0.766	0.034	0.343	0.351	−0.123	−0.138	−0.289	0.370	0.920	0.219	443	0.949
0.05	−3.740	0.812	0.036	−1.121	0.058	−0.004	−0.028	0.724	0.032	0.302	0.362	−0.140	−0.158	−0.205	0.370	0.940	0.239	435	0.940
0.075	−3.076	0.812	0.050	−1.252	0.121	−0.005	−0.051	0.648	0.040	0.243	0.333	−0.150	−0.196	−0.208	0.370	0.952	0.251	439	0.923
0.10	−2.661	0.812	0.060	−1.308	0.166	−0.009	−0.068	0.621	0.046	0.224	0.313	−0.146	−0.253	−0.258	0.370	0.958	0.257	439	0.901
0.15	−2.270	0.812	0.041	−1.324	0.212	−0.033	−0.081	0.613	0.031	0.318	0.344	−0.176	−0.267	−0.284	0.370	0.974	0.273	439	0.862
0.20	−2.771	0.812	0.030	−1.153	0.098	−0.014	−0.038	0.704	0.026	0.296	0.342	−0.148	−0.183	−0.359	0.370	0.981	0.280	439	0.844
0.30	−2.999	0.812	0.007	−1.080	0.059	−0.007	−0.022	0.752	0.007	0.359	0.385	−0.162	−0.157	−0.585	0.370	0.984	0.283	439	0.859
0.40	−3.511	0.812	−0.015	−0.964	0.024	−0.002	−0.005	0.842	−0.016	0.379	0.438	−0.078	−0.129	−0.557	0.370	0.987	0.286	439	0.871
0.50	−3.556	0.812	−0.035	−0.964	0.023	−0.002	−0.004	0.842	−0.036	0.406	0.479	−0.122	−0.130	−0.701	0.370	0.990	0.289	439	0.890
0.75	−3.709	0.812	−0.071	−0.964	0.021	−0.002	−0.002	0.842	−0.074	0.347	0.419	−0.108	−0.124	−0.796	0.331	1.021	0.320	438	0.917
1.0	−3.867	0.812	−0.101	−0.964	0.019	0	0	0.842	−0.105	0.329	0.338	−0.073	−0.072	−0.858	0.281	1.021	0.320	438	0.935
1.5	−4.093	0.812	−0.150	−0.964	0.019	0	0	0.842	−0.155	0.217	0.188	−0.079	−0.056	−0.954	0.210	1.021	0.320	428	0.960
2.0	−4.311	0.812	−0.180	−0.964	0.019	0	0	0.842	−0.187	0.060	0.064	−0.124	−0.116	−0.916	0.160	1.021	0.320	405	0.971
3.0	−4.817	0.812	−0.193	−0.964	0.019	0	0	0.842	−0.200	−0.079	0.021	−0.154	−0.117	−0.873	0.089	1.021	0.320	333	0.976
4.0	−5.211	0.812	−0.202	−0.964	0.019	0	0	0.842	−0.209	−0.061	0.057	−0.054	−0.261	−0.889	0.039	1.021	0.320	275	0.978
Vertical Component																			
Unc. PGA	−2.807	0.756	0	−1.391	0.191	0.044	−0.014	0.544	0	0.091	0.223	−0.096	−0.212	−0.199	0.630	1.003	0.302	941	0.964
Cor. PGA	−3.108	0.756	0	−1.287	0.142	0.046	−0.040	0.587	0	0.253	0.173	−0.135	−0.138	−0.256	0.630	0.975	0.274	439	0.958
0.05	−1.918	0.756	0	−1.517	0.309	0.069	−0.023	0.498	0	0.058	0.100	−0.195	−0.274	−0.219	0.630	1.031	0.330	434	0.934
0.075	−1.504	0.756	0	−1.551	0.343	0.083	0	0.487	0	0.135	0.182	−0.224	−0.303	−0.263	0.630	1.031	0.330	436	0.910
0.10	−1.672	0.756	0	−1.473	0.282	0.062	0.001	0.513	0	0.168	0.210	−0.198	−0.275	−0.252	0.630	1.031	0.330	436	0.900
0.15	−2.323	0.756	0	−1.280	0.171	0.045	0.008	0.591	0	0.223	0.238	−0.170	−0.175	−0.270	0.630	1.031	0.330	436	0.899
0.20	−2.998	0.756	0	−1.131	0.089	0.028	0.004	0.668	0	0.234	0.256	−0.098	−0.041	−0.311	0.571	1.031	0.330	436	0.915
0.30	−3.721	0.756	0.007	−1.028	0.050	0.010	0.004	0.736	0.007	0.249	0.328	−0.026	0.082	−0.265	0.488	1.031	0.330	436	0.941
0.40	−4.536	0.756	−0.015	−0.812	0.012	0	0	0.931	−0.018	0.299	0.317	−0.017	0.022	−0.257	0.428	1.031	0.330	436	0.949
0.50	−4.651	0.756	−0.035	−0.812	0.012	0	0	0.931	−0.043	0.243	0.354	−0.020	0.092	−0.293	0.383	1.031	0.330	436	0.957
0.75	−4.903	0.756	−0.071	−0.812	0.012	0	0	0.931	−0.087	0.295	0.418	0.078	0.091	−0.349	0.299	1.031	0.330	435	0.962
1.0	−4.950	0.756	−0.101	−0.812	0.012	0	0	0.931	−0.124	0.266	0.315	0.043	0.101	−0.481	0.240	1.031	0.330	435	0.967
1.5	−5.073	0.756	−0.150	−0.812	0.012	0	0	0.931	−0.184	0.171	0.211	−0.038	−0.018	−0.518	0.240	1.031	0.330	420	0.973
2.0	−5.292	0.756	−0.180	−0.812	0.012	0	0	0.931	−0.222	0.114	0.115	0.033	−0.022	−0.503	0.240	1.031	0.330	395	0.977
3.0	−5.748	0.756	−0.193	−0.812	0.012	0	0	0.931	−0.238	0.179	0.159	−0.010	−0.047	−0.539	0.240	1.031	0.330	321	0.978
4.0	−6.042	0.756	−0.202	−0.812	0.012	0	0	0.931	−0.248	0.237	0.134	−0.059	−0.267	−0.606	0.240	1.031	0.330	274	0.980

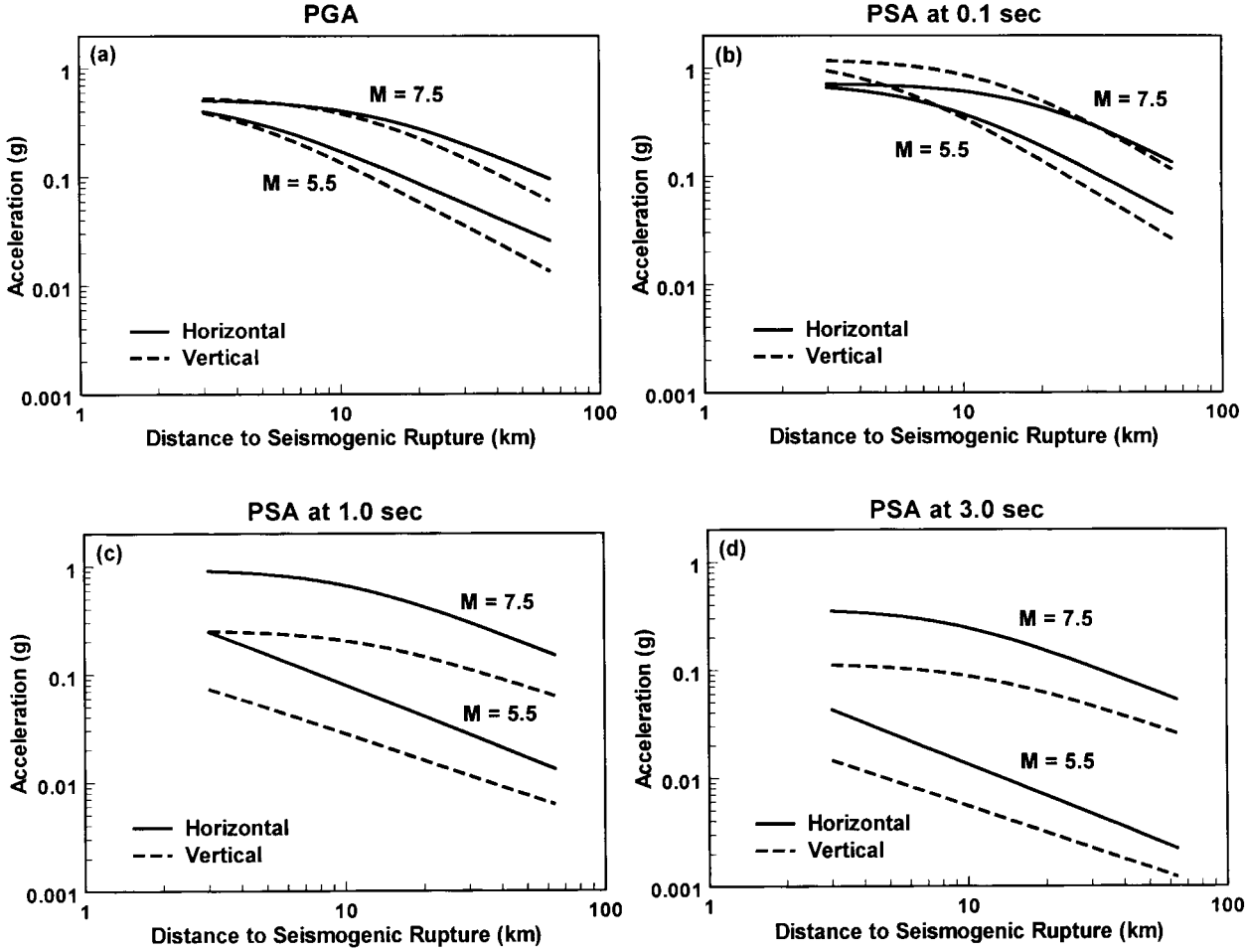

Figure 2. Ground-motion relations from this study for strike-slip faulting, firm soil, and the average horizontal (solid) and vertical (dashed) components of ground motion: (a) corrected PGA, (b) PSA at 0.1 sec, (c) PSA at 1.0 sec, and (d) PSA at 3.0 sec.

and 1994 Northridge blind-thrust earthquakes. This could be due to our combining blind and surface-rupturing earthquakes in the thrust-faulting category (Somerville, 2000), or it could simply be due to the fact that the Whittier Narrows and Northridge earthquakes have unusually large ground motion, even when compared to other thrust earthquakes. There is a greater opportunity for sites to be located over the hanging-wall of thrust faults than reverse faults, which increases their likelihood for higher ground motion at close distances. The relatively small difference in ground motion between reverse- and thrust-faulting events could also be due in part to a bias in the corrected database. This is suggested by comparing the values of the coefficients c_{10} and c_{11} in Table 4 between uncorrected and corrected PGA. The uncorrected PGA estimates for thrust faulting are 14% higher than for reverse faulting for both the horizontal and vertical components. On the other hand, the corrected PGA estimates for thrust faulting are only 1% higher than for reverse faulting (negligible) for the horizontal component and are actually 8% lower than for reverse faulting for the vertical component. Although their differences are relatively small and probably not statistically significant for all spectral ordinates, we chose to leave the reverse and thrust categories in our ground-motion relations to draw attention to their distinction. If the user does not believe that these categories are sufficient to warrant separate categories, they can combine the two categories by setting $F_{RV} = F_{TH} = 0.5$.

The regression models for the horizontal and vertical components of PGA and PSA were validated using an analysis of residuals. For purposes of this analysis, we defined a residual as

$$\delta_i = (\ln Y_i - \overline{\ln Y_i})/\sigma_{\ln(\text{Unc. PGA})}, \qquad (13)$$

where $\ln Y_i$ is the natural logarithm of the ith observed value of Y, $\overline{\ln Y_i}$ is the natural logarithm of the ith predicted value of Y, and $\sigma_{\ln(\text{Unc.PGA})}$ is the standard deviation of the natural logarithm of uncorrected PGA. The residuals were normalized by $\sigma_{\ln(\text{Unc, PGA})}$ in order to better visualize the relative differences in the scatter in the residuals among the different strong-motion parameters. For the model to be unbiased, the

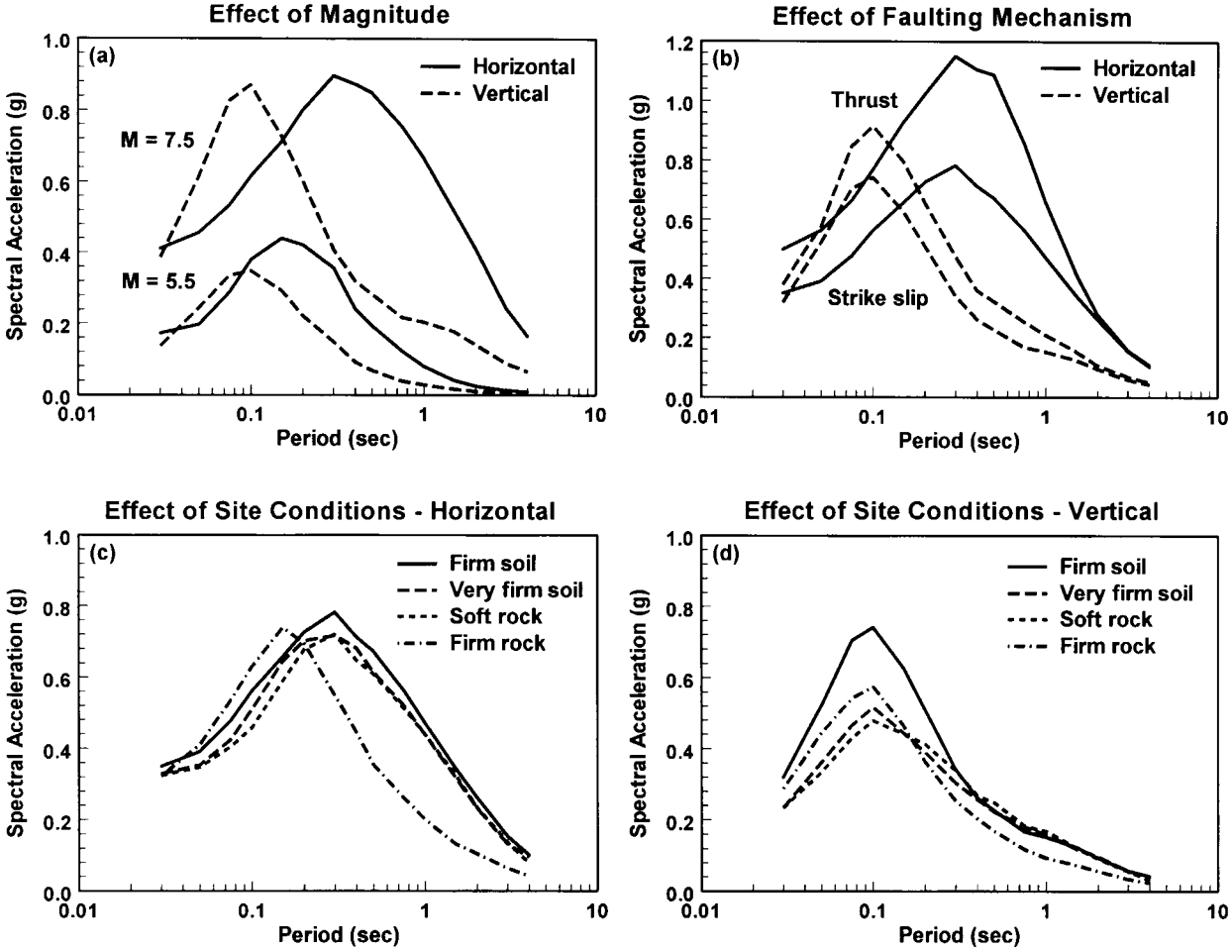

Figure 3. PSA (5% damping) predicted from the ground-motion relations developed in this study showing the effects of (a) magnitude, (b) faulting mechanism, (c) local soil conditions for the horizontal component of ground motion, and (d) local soil conditions for the vertical component of ground motion. Unless otherwise noted, the spectra are evaluated for M_W 7.0, r_{seis} = 10 km, strike-slip faulting, firm soil, and the average horizontal (solid line) and vertical (dashed line) components of ground motion. The reverse-faulting category has amplitudes that are approximately 10% lower than the thrust-faulting category, although this difference varies with period.

residuals should have zero mean and be uncorrelated with respect to the parameters in the regression model. Residual plots for the average horizontal component of ground motion as a function of magnitude and distance for selected response spectral ordinates are shown in Figures 4 and 5, respectively. These figures indicate that the regression models are unbiased with respect to these two parameters. Other plots show similarly unbiased results for faulting mechanism, site conditions, vertical components, and other natural periods (see Campbell and Bozorgnia, 2000a).

As a check on the consistency between the independent regression analyses of the horizontal and vertical components, we performed an analysis of residuals on the vertical-to-horizontal (V/H) response spectral ratio. This ratio was calculated from the equation

$$\ln(\text{V/H}) = \ln Y_V - \ln Y_H, \qquad (14)$$

where $\ln Y_V$ and $\ln Y_H$ were estimated from equations (1) through (10) using the regression coefficients listed in Table 4. A statistical estimate of the overall model bias, defined as the mean residual, is given in Table 5. This table indicates that the biases for PGA and PSA are all near zero, confirming that the predicted values of V/H from equation (14) are unbiased overall, even though they were calculated from independent regression analyses on the horizontal and vertical components of ground motion. The standard deviations of ln(V/H) listed in Table 5 are smaller than the standard deviations of either the average horizontal or the vertical components. This is the result of the strong statistical correlation between the horizontal and vertical ground-motion components and the fewer number of degrees of freedom (regression parameters) in the equation for ln(V/H). As one would expect from the unbiased residuals for the horizontal and vertical components, the residuals for V/H are also unbiased

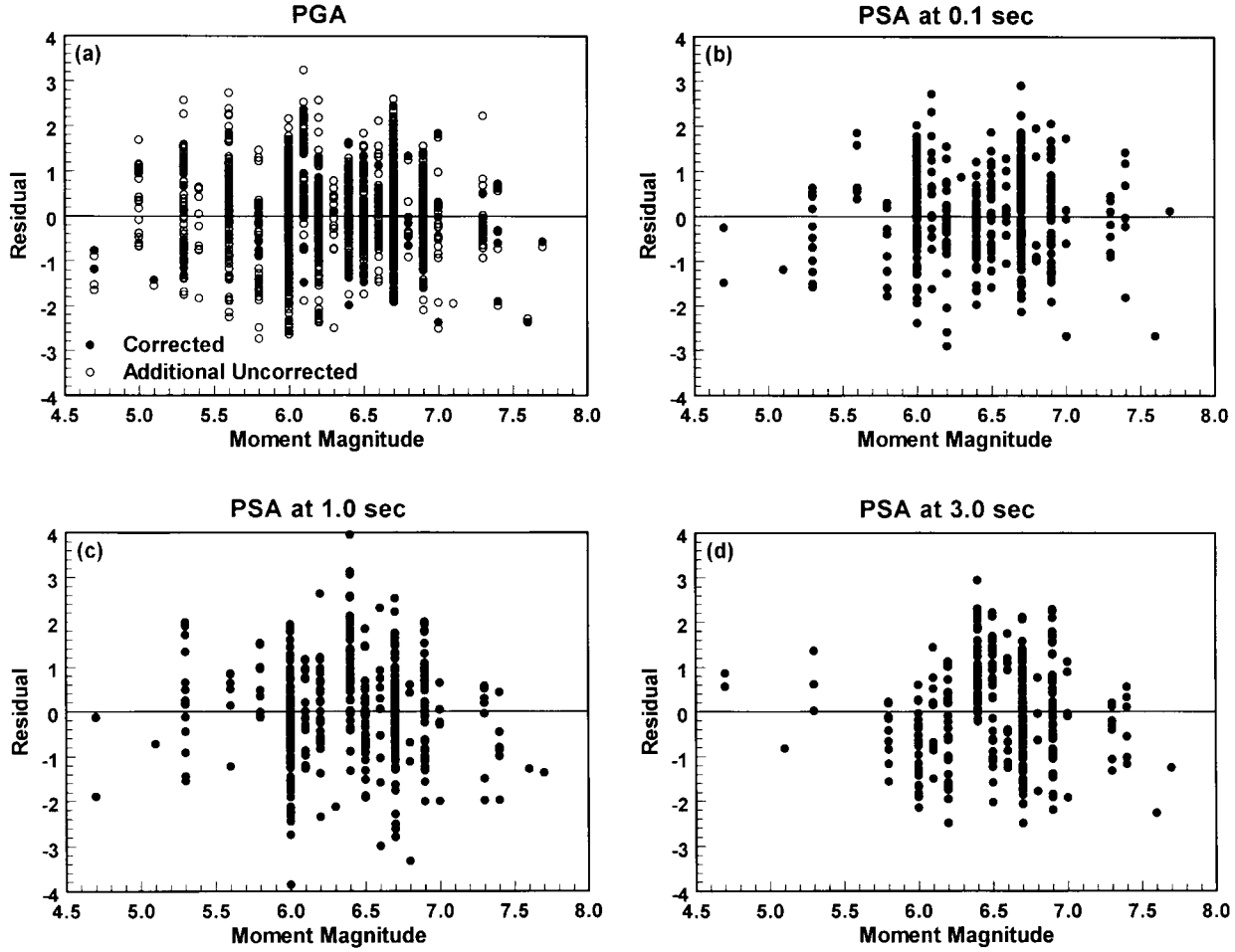

Figure 4. Ground-motion residuals as a function of magnitude for the regression analysis of the average horizontal component of ground motion: (a) corrected PGA (solid circles) and additional uncorrected PGA (open circles), (b) PSA at 0.1 sec, (c) PSA at 1.0 sec, and (d) PSA at 3.0 sec.

with respect to magnitude, distance, faulting mechanism, and site conditions (see Campbell and Bozorgnia, 2000a; Bozorgnia and Campbell, 2003). A complete discussion of the analysis of the V/H spectral ratio and its engineering implications is given by Bozorgnia and Campbell (2003).

Comparison with Previous Studies

We compared our new ground-motion relations with four ground-motion relations that are widely used to estimate horizontal response spectra for seismological and engineering analyses in nonextensional regions of western North America (Sadigh *et al.*, 1993, 1997; Abrahamson and Silva, 1997; Boore *et al.*, 1997; Campbell, 1997, 2000, 2001). The Sadigh *et al.* (1997) relation addresses the average horizontal component for both soil and rock. The Sadigh *et al.* (1993) relation addresses the horizontal and vertical components for rock only. Only the relations of Sadigh *et al.* (1993), Abrahamson and Silva (1997), and Campbell (1997, 2000, 2001) address the vertical component. All of these relations represent a seismically active, shallow-crustal tectonic environment, consistent with our study. They all define the faulting mechanism as either strike slip or reverse, where the latter includes both reverse and thrust faulting as defined in our study. They all use different definitions for local site conditions. Sadigh *et al.* (1993, 1997) claimed that their relations for rock include sites with no more than 1 m of soil overlying rock; however, B. Youngs (personal comm., 2002) has suggested that this is not strictly true and that the rock sites include thicker layers of soil, possibly up to 20 m. The Sadigh *et al.* (1997) relation for soil includes sites with greater than 20 m of soil overlying rock. The Abrahamson and Silva (1997) relation uses the soil definition of Sadigh *et al.* (1993, 1997) and defines rock as a deposit with less than 20 m of soil overlying rock. It differentiates between these two categories using an amplitude-dependent site factor. The Boore *et al.* (1997) relation accounts for site effects using the velocity parameter, V_{S30}. According to Boore and Joyner (1997), sites classified as generic soil, as defined by Boore *et al.* (1997), are consistent with a 30-m velocity of

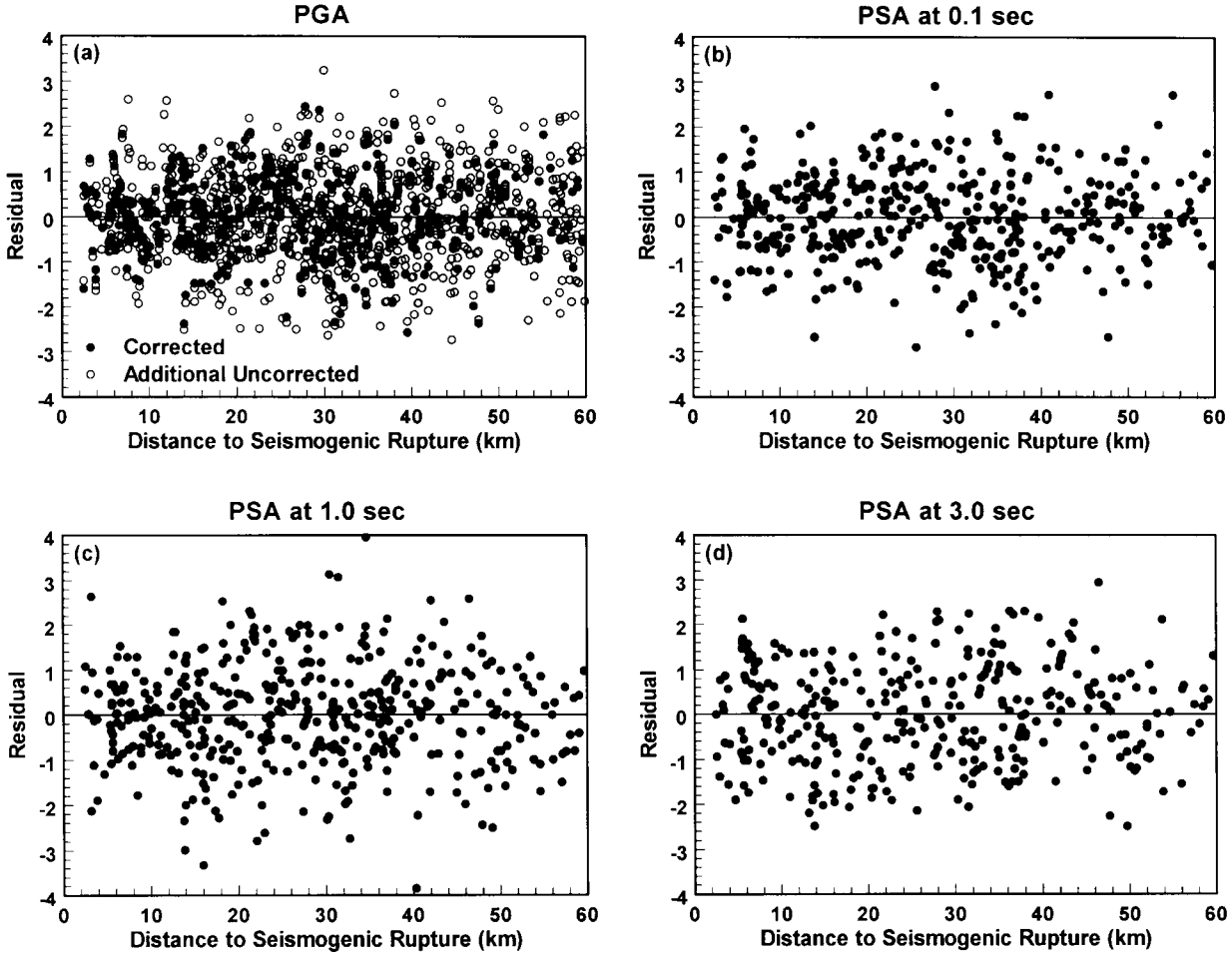

Figure 5. Ground-motion residuals as a function of distance for the regression analysis of the average horizontal component of ground motion: (a) corrected PGA (solid circles) and additional uncorrected PGA (open circles), (b) PSA at 0.1 sec, (c) PSA at 1.0 sec, and (d) PSA at 3.0 sec.

Table 5
Bias in Predicted Value of Vertical-to-Horizontal (V/H) Ratio

Period (sec)	No.	Bias in ln (V/H)	Bias (Factor)	$\sigma_{\ln V/H}$
Unc. PGA	941	−0.0121	0.99	0.432
Cor. PGA	439	−0.0074	0.99	0.422
0.05	432	0.0003	1.00	0.465
0.075	436	−0.0081	0.99	0.470
0.10	436	−0.0098	0.99	0.469
0.15	436	−0.0110	0.99	0.493
0.20	436	−0.0100	0.99	0.480
0.30	436	−0.0094	0.99	0.463
0.40	436	−0.0074	1.00	0.483
0.50	436	−0.0044	1.00	0.491
0.75	435	−0.0057	0.99	0.487
1.0	435	−0.0033	1.00	0.514
1.5	419	−0.0183	0.98	0.487
2.0	393	−0.0292	0.97	0.454
3.0	313	−0.0370	0.96	0.437
4.0	262	0.0055	1.01	0.451

about 310 m/sec, and sites classified as generic rock are consistent with a 30-m velocity of about 620 m/sec. The Campbell (1997, 2000, 2001) relation classifies sites as generic soil, soft rock, or hard rock. Campbell (2002, 2003) presents a more thorough summary of all four of these ground-motion relations and suggests adjustments that make them more consistent with the definition of generic soil and generic rock given previously. For the evaluation given here, we did not make any adjustments to be consistent with current engineering practice.

Figures 6 and 7 compare the predicted median spectral acceleration from the four selected ground-motion relations with that predicted from our ground motion relations for a site located 10 km from a strike-slip earthquake of M_W 7.0. This distance corresponds to $r_{jb} = r_{rup} = 10$ km and $r_{seis} = 10.4$ km, assuming the fault ruptures to the surface and that the depth to seismogenic rupture is 3 km (Abrahamson and Shedlock, 1997; Campbell, 2002, 2003). r_{rup} is the distance measure used by Abrahamson and Silva (1997) and Sadigh *et al.* (1993, 1997) and represents the closest distance

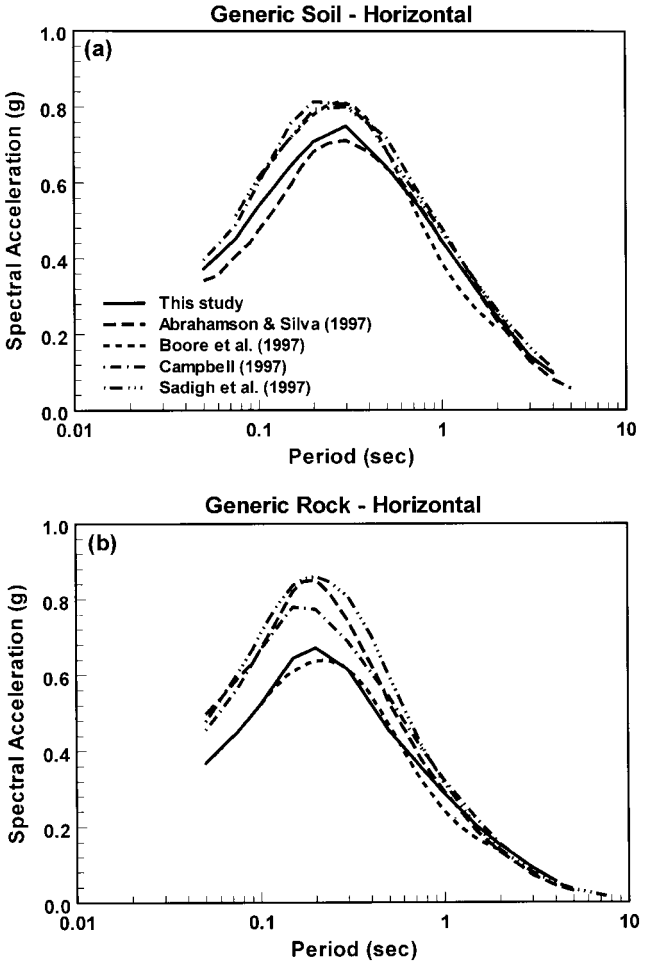

Figure 6. Comparison of predicted PSA (5% damping) from the horizontal ground-motion relation in this study and four ground-motion relations widely used in seismology and engineering: (a) generic soil, (b) generic rock. Generic soil and rock are defined in the text but generally represent sites with V_{S30} = 310 and 620 m/sec, respectively, although these velocities will vary depending on the specific relation. The spectra are evaluated for M_W 7.0, r_{jb} = r_{rup} = 10 km, r_{seis} = 10.4 km, and vertical strike-slip faulting.

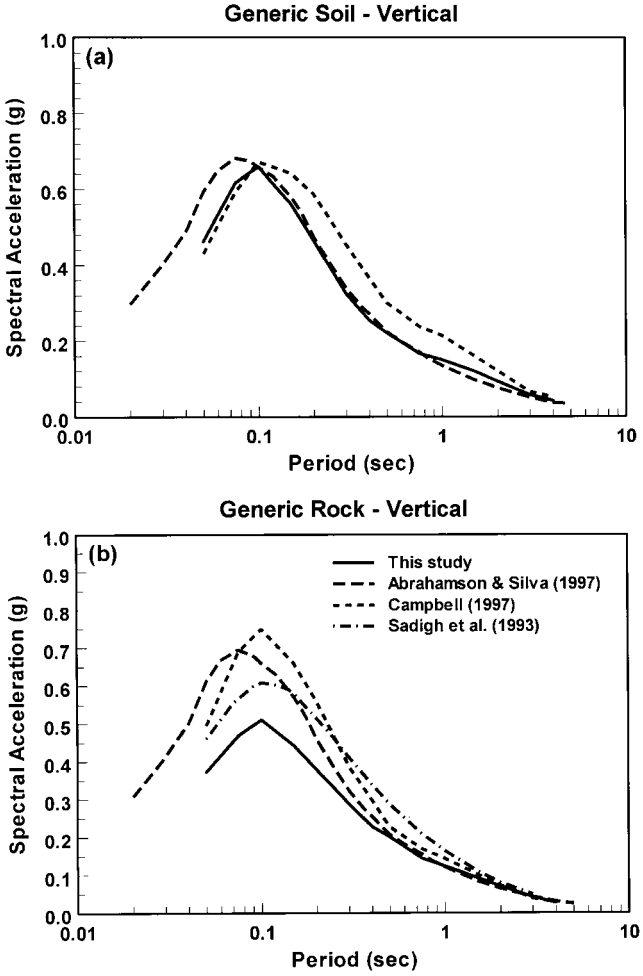

Figure 7. Comparison of predicted PSA (5% damping) from the vertical ground-motion relation in this study and three ground-motion relations widely used in seismology and engineering: (a) generic soil, (b) generic rock. Generic soil and rock are defined in the text but generally represent sites with V_{S30} = 310 and 620 m/sec, respectively, although these velocities will vary depending on the specific relation. The spectra are evaluated for M_W 7.0, r_{jb} = r_{rup} = 10 km, r_{seis} = 10.4 km, and vertical strike-slip faulting.

to fault rupture. Comparisons are shown for the two most common site conditions used in engineering analysis, namely, generic soil and generic rock. Our ground-motion relation was evaluated for generic soil by setting S_{VFS} = 0.25 and S_{SR} = S_{FR} = 0 and for generic rock by setting S_{VFS} = 0 and S_{SR} = S_{FR} = 0.5. These values represent the approximate proportion of recordings in our database that comprise each of these categories. The Campbell (1997, 2000, 2001) ground-motion relation was evaluated for generic soil by setting S_{SR} = S_{HR} = 0 and D = 5 km and for generic rock by setting S_{SR} = 1, S_{HR} = 0, and D = 1 km (Campbell, 2001). The Boore *et al.* (1997) relation was evaluated for generic soil and generic rock by setting V_{S30} = 310 m/sec and V_{S30} = 620 m/sec, respectively (Boore and Joyner, 1997). The other ground-motion relations were evaluated for generic soil and generic rock using their soil and rock categories.

The comparison in Figures 6 (horizontal component) and 7 (vertical component) shows that our relations predict spectral accelerations that are generally similar to those of the other four ground-motion relations when evaluated for generic soil and generic rock. The least variability among the models occurs for the horizontal component on generic soil. This is no surprise, since this category contains the largest number of recordings. Our ground-motion relations predict relatively low amplitudes at short periods for the horizontal component on generic rock, consistent with that of Boore *et al.* (1997). It is interesting to note that the Boore *et al.* (1997) relation is the only one that is specifically eval-

uated for $V_{S30} = 620$ m/sec, the *de facto* definition of generic rock. This same trend is seen in the spectra for the vertical component of generic rock. In general, there is more variability among the ground-motion relations for the vertical component, reflecting in part its greater aleatory variability (Fig. 8b), which allows a wider mathematical interpretation of the data. Because of the relatively large differences in ground motion for the site categories defined in our study, the comparison in Figures 6 and 7 would not be so favorable for some of our other site conditions. This is especially true for very firm soil, which comprises only about 25% of the generic soil category but behaves similarly to soft rock, and for firm rock, which comprises 50% of the generic rock category but behaves significantly different from soft rock, especially at long periods. Only Boore *et al.* (1997) addressed these differences by virtue of their site parameter, V_{S30}, but they did not incorporate nonlinear site effects.

Figure 8 shows a comparison of the standard deviations (natural log) predicted from the ground-motion relations evaluated in Figures 6 and 7. The standard deviation is important because it contributes significantly to deterministic estimates of ground motion that are defined by the median plus one standard deviation and to probabilistic estimates of ground motion, especially at long return periods, where $\sigma_{\ln Y}$ can increase the predicted ground motion by a factor of 2 to 3, depending on its value. Figure 8 indicates that our horizontal standard deviations are among the lowest and that our vertical standard deviations are the lowest among those ground-motion relations evaluated. Note that the horizontal standard deviations of Boore *et al.* (1997) are independent of magnitude and plot among those for M_W 7.5 in Figure 8a.

Figure 9 compares the attenuation characteristics of PGA predicted by the ground-motion relations evaluated in Figures 6 and 7 for a suite of sites located on the hanging wall of a 45°-dipping thrust fault. The event is intentionally large (M_W 7.5), and PGA is plotted on a linear scale to accentuate the hanging-wall effects. All of the relations are plotted versus the distance measure, r_{rup}, for purposes of comparison. Only our updated relation and that of Abrahamson and Silva (1997) explicitly include hanging-wall effects. The Boore *et al.* (1997) relation inherently includes hanging-wall effects by virtue of its distance measure, r_{jb}. The value of PGA predicted by the Campbell (1997) relation decreases at very small values of r_{rup} once its distance measure, r_{seis}, begins to increase past the point at which the top of the 3-km seismogenic depth on the fault is reached. Our relation would do the same, except that the hanging-wall effects keep it approximately constant at these small distances. Our generic rock results are similar to those of Abrahamson and Silva (1997), except at $r_{rup} < 4$ km, where our predictions remain constant and theirs begin to increase. Although the Boore *et al.* (1997) predictions show similar behavior, the constant part of the curve occurs at a much smaller value of PGA. Our generic soil results show a small effect of the hanging wall because of the 25% weight given to very firm soil (remember that there are no additional hanging-wall effects for firm soil). The Abrahamson and Silva (1997) relation shows more subdued hanging-wall effects because of nonlinear soil behavior. In the case of generic soil, the Boore *et al.* (1997) relation predicts much higher PGA, possibly due to a lack of nonlinear effects.

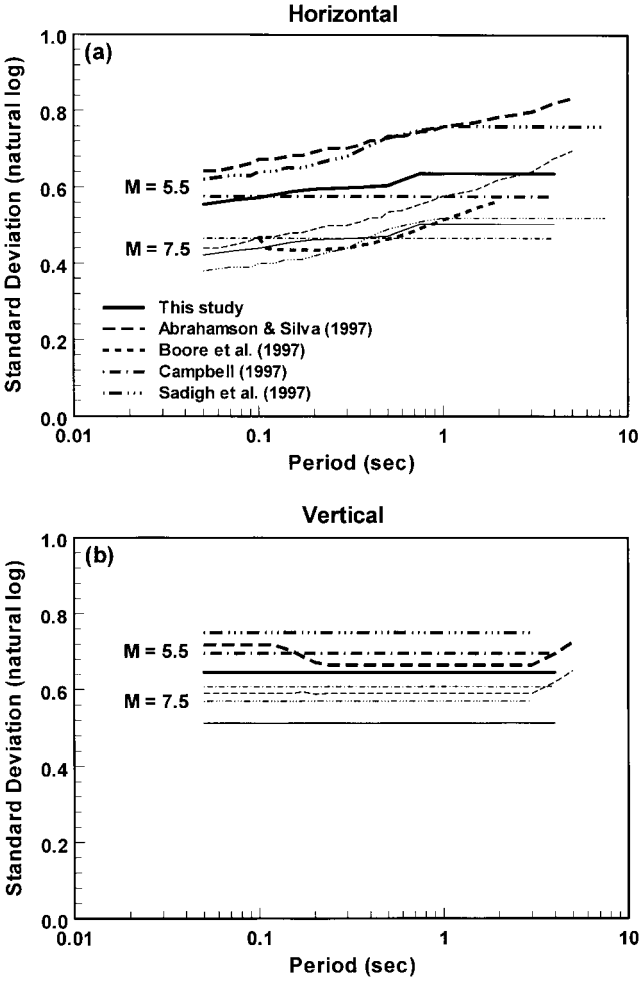

Figure 8. Comparison of predicted standard deviations of spectral acceleration ($\sigma_{\ln Y}$) from this study and four ground-motion relations widely used in seismology and engineering: (a) average horizontal component, (b) vertical component. The standard deviations are evaluated for M_W 5.5 (thick lines) and M_W 7.5 (thin lines). The standard deviations from this study are calculated from the $\sigma_{\ln Y}$ versus M_W relationship. Those from Sadigh *et al.* (1997) are calculated from their rock relation.

Recommendations and Conclusions

We consider the ground-motion relations developed in this study to be valid for estimating PGA and 5%-damped PSA for earthquakes of $M_W \geq 5.0$ and distances of $r_{seis} \leq 60$ km for shallow crustal earthquakes in western North America and in similar seismically active tectonic regimes worldwide. The relations can be extrapolated to a distance of

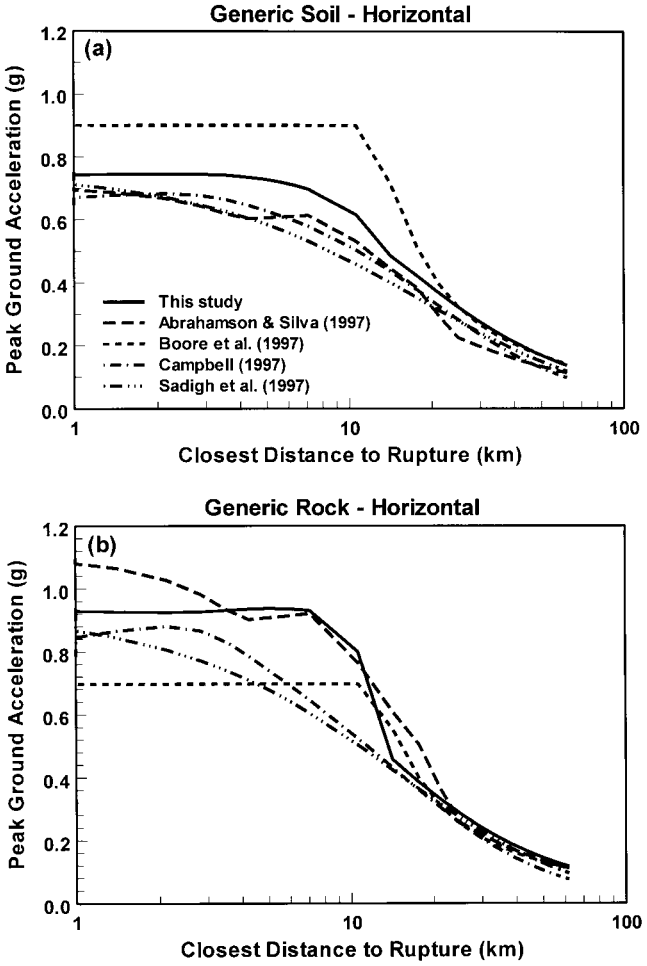

Figure 9. Comparison of predicted PGA on the hanging wall between this study and four horizontal ground-motion relations widely used in seismology and engineering: (a) generic soil, (b) generic rock. Generic soil and rock are defined in the text but generally represent sites with $V_{S30} = 310$ and 620 m/sec, respectively, although these velocities will vary depending on the specific relation. The relations are evaluated for M_W 7.5 and for a reverse or thrust fault dipping at 45°. PGA is plotted on a linear scale to emphasize the differences in the relations at short distances. Besides this study, only the Abrahamson and Silva (1997) relation includes an explicit parameter for hanging-wall effects. The Boore *et al.* (1997) relation includes apparent hanging-wall effects by nature of their distance measure (see text). The more subdued effect of the hanging wall for generic soil in this study is due to the 75% weight given to firm soil, which does not include hanging-wall effects.

100 km without serious compromise, but like all of the empirical models evaluated in this article, they should not be used beyond this distance without carefully considering the possible engineering consequences. For example, like many of the other relations, our relations overpredict ground motion beyond 100 km and, therefore, provide a conservative engineering estimate of ground motion at these distances.

We consider our updated ground-motion relations to supersede our previous relations (Campbell and Bozorgnia, 1994; Campbell, 1997, 2000, 2001), except when sediment depth needs to be evaluated, which is not included in our updated relations. Although there was a limited attempt to smooth the trends in the regression coefficients of our updated ground-motion relations, the resulting spectra still exhibit some period-to-period variability. Therefore, we recommend that the ground motion predicted from these relations be averaged with that from other credible ground-motion relations when calculating engineering estimates of ground motion, consistent with the common engineering practice of incorporating epistemic variability. We provide some guidance on how to evaluate our updated ground-motion relations for different site conditions and faulting mechanisms in Tables 6 and 7. Table 6 includes an estimate of the expected range of V_{S30} along with the approximate NEHRP site class (Wills *et al.*, 2000) for the four site categories defined in this study to aid in the selection of an appropriate site category to use when evaluating the model. Since the range of V_{S30} for firm rock has a mean that is higher than that corresponding to the NEHRP BC boundary (760 m/sec) used to define the reference site condition in the USGS seismic hazard maps, we recommend that horizontal ground motion for this latter site condition be calculated from our generic rock prediction by applying an appropriate amplification factor from Boore *et al.* (1997). This factor can be calculated from the expression $\exp[b_V \ln(620/760)]$, where b_V is the period-dependent coefficient representing the relationship between ground motion and V_{S30}.

It is important to recognize that this study was intended to be a limited update of the ground-motion relations developed by Campbell and Bozorgnia (1994) and Campbell (1997, 2000, 2001), with the explicit purpose of providing engineers and seismologists with a mutually consistent set of near-source ground-motion relations to use in seismic hazard analysis. It should be noted that the USGS and the CGS have selected our updated ground-motion relation as one of several that they are using in their 2002 revision of the U.S. and California seismic hazard maps (Frankel *et al.*, 2002). Being a limited update, the study does not explicitly address such topics as PGV, sediment depth, rupture directivity effects, or the use of the 30-m velocity or related NEHRP site classes. These topics are the subject of ongoing research and will be addressed in a future update. We do, however, refine some of the parameters previously used by Campbell (1997, 2000, 2001) by including hanging-wall effects, by dividing their reverse-faulting events into reverse- and thrust-faulting categories, and by dividing their generic-soil site class into firm and very firm soil categories. We retained the use of their soft rock and hard rock categories, though we renamed the latter "firm rock" to avoid confusion with the hard rock units of eastern North America.

Based on the empirical analysis performed in this study, we offer the following specific observations and conclusions:

Table 6
Guidance on Evaluating Ground-Motion Relations for Local Site Conditions

Site Category	Site Parameter S_{VFS}	Site Parameter S_{SR}	Site Parameter S_{FR}	Approximate V_{S30} (m/sec)*	Approximate Site Class†
Firm soil	0.00	0.00	0.00	210–390	D
Very firm soil	1.00	0.00	0.00	290–490	CD
Soft rock	0.00	1.00	0.00	310–530	CD
Firm rock	0.00	0.00	1.00	490–1170	BC
Generic soil	0.25	0.00	0.00	≈310	D
Generic rock	0.00	0.50	0.50	≈620	C
BC boundary	0.00	0.50	0.50	760	BC
	[then add b_v ln(620/760)]‡				

*Approximate one-standard deviation range from Wills and Silva (1998) for similar geologic units.
†Site classes defined by Wills *et al.* (2000).
‡Term comes from Boore *et al.* (1997) and should be added to ln *Y*.

Table 7
Guidance on Evaluating Ground-Motion Relations for Faulting Mechanism

Faulting Category	Faulting Parameter F_{RV}	Faulting Parameter F_{TH}
Strike slip or normal	0.00	0.00
Reverse	1.00	0.00
Thrust	0.00	1.00
Reverse or thrust	0.50	0.50
Generic (unknown)	0.25	0.25

1. We found the common practice of using generic soil and generic rock to define local site conditions to be too simplistic. We found the seismic behavior of very firm soil, the stiffer component of generic soil, to be closer to that of soft rock than to that of firm soil, the softer component of generic soil. Furthermore, we found the seismic behavior of firm rock, the harder component of generic rock, to be significantly different from that of soft rock, the softer component of generic rock. These observations are consistent with the approximate range of 30-m velocity for these site categories given in Tables 3 and 6. Of the four site categories considered, we found apparent strong nonlinear behavior only for the short-period, horizontal component of ground motion on firm soil, probably because of its lower stiffness and its greater likelihood of being saturated. The vertical component of ground motion appeared not to be affected by nonlinear site effects. Although not addressed in our study, other studies have also shown soft soil to have significant nonlinear site effects.
2. We found the greatest differences in median predicted horizontal ground motion among the four site categories defined in this study to occur at long periods on firm rock, which had significantly lower amplitudes due to an absence of sediment amplification, and at short periods on firm soil, which had relatively low amplitudes at large magnitudes and short distances due to nonlinear site effects. Vertical ground motion showed similar behavior for firm rock at long periods but had relatively high short-period amplitudes on firm soil due to a combination of a lack of nonlinear site effects, less anelastic attenuation, and phase conversions within the upper sediments (Silva, 1997; Amirbekian and Bolt, 1998; Bozorgnia and Campbell, 2003).
3. We found differences in median-predicted spectral acceleration among strike-slip, reverse, and thrust-faulting earthquakes to be consistent with differences in dynamic stress drop. These differences were found to become negligible at periods of 2 sec and greater, where dynamic stress drop is expected to have little impact on the amplitude of strong ground motion. This result could help to explain the large ground motion observed during several recent blind-thrust earthquakes, which have been shown from independent seismological studies to have relatively large dynamic stress drop. The relatively small (less than 10%) differences in median-predicted ground motion between reverse- and thrust-faulting earthquakes are not consistent with the hypothesis that all thrust faults have unusually high ground motions. There are, however, more opportunities for hanging-wall effects on the shallower-dipping thrust faults, which will lead to a greater number of sites with relatively high ground motion as compared to the more steeply dipping reverse faults. Furthermore, there are also several statistical reasons, listed in the text, that could have caused this result. We conclude that additional study is needed to determine exactly what additional earthquake source characteristics can be expected to result in higher ground motions from thrust (especially blind-thrust) faults.
4. We found that the model for hanging-wall effects given by Abrahamson and Silva (1997) could also be used with our ground-motion relations. However, we restricted the definition of the hanging wall to be that part of the crust over the rupture plane, with a 5-km margin defined in terms of the distance measure, r_{jb}, to allow for a smooth transition from hanging-wall to no hanging-wall effects.

We also found that hanging-wall effects were not significant for firm soil sites, whose ground-motion amplitudes at short distances and large magnitudes had apparently already reached the limit allowed by nonlinear site effects.

5. Based on an analysis of residuals, we found sediment depth (depth to basement rock) to have a significant effect on the amplitude of ground motion, especially at long periods. This effect was greatest for the horizontal component of ground motion. Sediment depth was not included as a parameter because its effect, especially its correlation with other parameters in the model, is not yet well understood. Furthermore, its exclusion is not a practical limitation, since it is typically not used in engineering analyses and it is not included in any other ground-motion relation widely used in engineering or seismology. However, it will be included as a parameter in the future once its mathematical form is better understood.
6. An analysis of residuals determined that the median value of the V/H response spectral ratio predicted from our updated vertical and horizontal ground-motion relations were unbiased with respect to magnitude, distance, faulting mechanism, and site conditions. This indicates that these relations are mutually consistent and, therefore, can be used to develop engineering estimates of horizontal and vertical ground motion.
7. Due to its statistical robustness, the ground-motion relation for uncorrected PGA should be used to estimate PGA only when an estimate of PGA is required (e.g., for liquefaction analysis). When an estimate of spectral acceleration is required, peak ground acceleration should be predicted from the ground-motion relation for corrected PGA to be consistent with the corresponding estimates of spectral acceleration.

Acknowledgments

This study was supported by the California Department of Conservation, Division of Mines and Geology (now the California Geological Survey), Strong-Motion Instrumentation Program, Contract 1097-606. We would also like to acknowledge the support of ABS Consulting, Inc., through its subsidiary EQECAT, Inc. We want to thank Steve Harmsen and an anonymous reviewer for their insightful comments, which significantly improved the manuscript. We would also like to acknowledge helpful discussions with Dave Boore and Ned Field during the course of the study.

References

Abrahamson, N. A., and K. M. Shedlock (1997). Overview, *Seism. Res. Lett.* **68,** 9–23.

Abrahamson, N. A., and W. J. Silva (1997). Empirical response spectral attenuation relations for shallow crustal earthquakes, *Seism. Res. Lett.* **68,** 94–127.

Akkar, S., and P. Gulkan (2002). A critical examination of near-field accelerograms from the Sea of Marmara region earthquakes, *Bull. Seism. Soc. Am.* **92,** 428–447.

Amirbekian, R. V., and B. A. Bolt (1998). Spectral comparison of vertical and horizontal seismic strong ground motions in alluvial basins, *Earthquake Spectra* **14,** 573–595.

Anderson, J. G. (2000). Expected shape of regressions for ground motion parameters on rock, *Bull. Seism. Soc. Am.* **90,** S43–S52.

Anderson, J. G. (2003). Strong motion seismology, in *International Handbook of Earthquake and Engineering Seismology*, W. H. K. Lee, H. Kanamori, P. C. Jennings, and C. Kisslinger (Editors), Academic Press, London, Vol. 2, Chapter 57.

Anderson, J. G., J. Sucuoglu, A. Erbernik, T. Yilmaz, E. Inan, E. Durukal, M. Erdik, R. Anooshehpoor, J. N. Brune, and S. D. Ni (2000). Implications for seismic hazard analysis, in *Kocaeli, Turkey, Earthquake of August 17, 1999, Reconnaissance Report*, T. L. Youd, J. P. Bardet, and J. D. Bray, (Editors), *Earthquake Spectra* **16** (Suppl. A), 113–137.

Atakan, K., A. Ojeda, M. Meghraoui, A. A. Barka, M. Erdik, and A. Bodare (2002). Seismic hazard in Istanbul following the 17 August 1999 Izmit and 12 November Duzce earthquakes, *Bull. Seism. Soc. Am.* **92,** 466–482.

Atkinson, G. M., and D. M. Boore (1998). Evaluation of models for earthquake source spectra in eastern North America, *Bull. Seism. Soc. Am.* **88,** 917–934.

Boore, D. M. (2001). Comparisons of ground motions from the 1999 Chi-Chi earthquake with empirical predictions largely based on data from California, *Bull. Seism. Soc. Am.* **91,** 1212–1217.

Boore, D. M., and W. B. Joyner (1997). Site amplification for generic rock sites, *Bull. Seism. Soc. Am.* **87,** 327–341.

Boore, D. M., W. B. Joyner, and T. E. Fumal (1997). Equations for estimating horizontal response spectra and peak acceleration from western North American earthquakes: a summary of recent work, *Seism. Res. Lett.* **68,** 128–153.

Bozorgnia, Y., and K. W. Campbell (2003). Vertical-to-horizontal response spectral ratio and the vertical design spectrum, *Earthquake Spectra* (submitted).

Bozorgnia, Y., K. W. Campbell, and M. Niazi (1999). Vertical ground motion: Characteristics, relationship with horizontal component, and building-code implications, in *Proc. SMIP99 Seminar on Utilization of Strong-Motion Data*, California Strong Motion Instrumentation Program, Sacramento, California, 23–49.

Campbell, K. W. (1989). Empirical prediction of near-source ground motion for the Diablo Canyon Power Plant Site, San Luis Obispo County, California, *U.S. Geol. Surv. Open-File Rept. 89–484.*

Campbell, K. W. (1991). An empirical analysis of peak horizontal acceleration for the Loma Prieta, California, earthquake of 18 October 1989, *Bull. Seism. Soc. Am.* **81,** 1838–1858.

Campbell, K. W. (1997). Empirical near-source attenuation relationships for horizontal and vertical components of peak ground acceleration, peak ground velocity, and pseudo-absolute acceleration response spectra, *Seism. Res. Lett.* **68,** 154–179.

Campbell, K. W. (1998). Empirical analysis of peak horizontal acceleration, peak horizontal velocity, and modified Mercalli intensity, in *The Loma Prieta, California, Earthquake of October 17, 1989—Earth Structures and Engineering Characterization of Ground Motion*, T. L. Holzer, (Editor), *U.S. Geol. Surv. Profess. Pap. 1552-D*, D47–D68.

Campbell, K. W. (2000). Erratum: empirical near-source attenuation relationships for horizontal and vertical components of peak ground acceleration, peak ground velocity, and pseudo-absolute acceleration response spectra, *Seism. Res. Lett.* **71,** 353–355.

Campbell, K. W. (2001). Erratum: empirical near-source attenuation relationships for horizontal and vertical components of peak ground acceleration, peak ground velocity, and pseudo-absolute acceleration response spectra, *Seism. Res. Lett.* **72,** 474.

Campbell, K. W. (2002). Engineering models of strong ground motion, in *Earthquake Engineering Handbook*, W. F. Chen and C. Scawthorn (Editors), CRC Press, Boca Rotan, Florida, Chapter 5-1–5-76.

Campbell, K. W. (2003). Strong motion attenuation relationships, in *Inter-*

national Handbook of Earthquake and Engineering Seismology W. H. K. Lee, H. Kanamori, P. C. Jennings, and C. Kisslinger (Editors), Academic Press, London, Vol. 2, Chapter 60.

Campbell, K. W., and Y. Bozorgnia (1994). Near-source attenuation of peak horizontal acceleration from worldwide accelerograms recorded from 1957 to 1993, in *Proc. 5th U.S. National Conference on Earthquake Engineering*, Earthquake Engineering Research Institute, Oakland, California, Vol. III, 283–292.

Campbell, K. W., and Y. Bozorgnia (2000a). Vertical ground motion: characteristics, relationship with horizontal component, and building-code implications, Contract Number 1097-606, Final Report, Prepared for the California Strong-Motion Instrumentation Program, Sacramento, California.

Campbell, K. W., and Y. Bozorgnia (2000b). New empirical models for predicting near-source horizontal, vertical, and V/H response spectra: implications for design, in *Proc. 6th International Conference on Seismic Zonation*, Earthquake Engineering Research Institute, Oakland, California (CD-ROM).

Chang, T. Y., F. Cotton, J. Angelier (2001). Seismic attenuation and peak ground acceleration in Taiwan, *Bull. Seism. Soc. Am.* **91,** 1229–1246.

Field, E. H. (2000). A modified ground motion attenuation relationship for southern California that accounts for detailed site classification and a basin-depth effect, *Bull. Seism. Soc. Am.* **90,** S209–S221.

Field, E. H., and the SCEC Phase III Working Group (2000). Accounting for site effects in probabilistic seismic hazard analyses of southern California: overview of the SCEC Phase III Report, *Bull. Seism. Soc. Am.* **90,** S1–S31.

Frankel, A. D., M. D. Petersen, C. S. Mueller, K. M. Haller, R. L. Wheeler, E. V. Leyendecker, R. L. Wesson, S. C. Harmsen, C. H. Cramer, D. M. Perkins, and K. S. Rukstales (2002). Documentation of the 2002 update of the national seismic hazard maps, *U.S. Geol. Surv. Open-File Rept. 02-420.*

Joyner, W. B. (2000). Strong motion from surface waves in deep sedimentary basins, *Bull. Seism. Soc. Am.* **90,** S95–S112.

Lee, Y, and J. G. Anderson (2000). Potential for improving ground motion relations in southern California by incorporating various site parameters, *Bull. Seism. Soc. Am.* **90,** S170–S186.

Olsen, K. B. (2000). Site amplification in the Los Angeles basin from three-dimensional modeling of ground motion, *Bull. Seism. Soc. Am.* **90,** S77–S94.

Park, S., and S. Elrick (1998). Predictions of shear-wave velocities in southern California using surface geology, *Bull. Seism. Soc. Am.* **88,** 677–685.

Sadigh, K., C. Y. Chang, N. A. Abrahamson, S. J. Chiou, and M. S. Power (1993). Specification of long-period ground motions: updated attenuation relationships for rock site conditions and adjustment factors for near-fault effects, in *Proc. ATC-17-1 Seminar on Seismic Isolation, Passive Energy Dissipation, and Active Control*, ATC-17-1, Applied Technology Council, Vol. 1, 59–70.

Sadigh, K., C. Y. Chang, J. A. Egan, F. Makdisi, and R. R. Youngs (1997). Attenuation relationships for shallow crustal earthquakes based on California strong motion data, *Seism. Res. Lett.* **68,** 180–189.

Silva, W. (1997). Characteristics of vertical strong ground motions for applications to engineering design, in *Proc. FHWA/NCEER Workshop on the National Representation of Seismic Ground Motion for New and Existing Highway Facilities*, Tech. Rept. NCEER-97-0010, National Center for Earthquake Engineering Research, Buffalo, New York.

Somerville, P. (2000). New developments in seismic hazard estimation. in *Proc. 6th International Conference on Seismic Zonation*, Earthquake Engineering Research Institute, Oakland, California, 25 pp. (CD-ROM).

Somerville, P., and J. Yoshimura (1990). The influence of critical MOHO reflections on strong ground motions recorded in San Francisco and Oakland during the 1989 Loma Prieta earthquake, *Geophys. Res. Lett.* **17,** 1203–1206.

Spudich, P., W. B. Joyner, A. G. Lindh, D. M. Boore, B. M. Margaris, and J. B. Fletcher (1999). SEA99: a revised ground motion prediction relation for use in extensional tectonic regimes, *Bull. Seism. Soc. Am.* **89,** 1156–1170.

Stewart, J. P. (2000). Variations between foundation-level and free-field earthquake ground motions, *Earthquake Spectra* **16,** 511–532.

Trifunac, M. D., and V. W. Lee (1989). Empirical models for scaling pseudo relative velocity spectra of strong earthquake accelerations in terms of magnitude, distance, site intensity and recording site conditions, *Soil Dyn. Earthquake Eng.* **8,** 126–144.

Trifunac, M. D., and V. W. Lee (1992). A note on scaling peak acceleration, velocity and displacement of strong earthquake shaking by Modified Mercalli Intensity (MMI) and site soil and geologic conditions, *Soil Dyn. Earthquake Eng.* **11**, 101–110.

Tsai, Y. B., and M. W. Huang (2000). Strong ground motion characteristics of the Chi-Chi, Taiwan earthquake of September 21, 1999, *Earthquake Eng. Eng. Seism.* **2,** 1–21.

Wills, C. J., and W. J. Silva (1998). Shear-wave velocity characteristics of geologic units in California, *Earthquake Spectra* **14,** 533–556.

Wills, C. J., M. Petersen, W. A. Bryant, M. Reichle, G. J. Saucedo, S. Tan, G. Taylor, and J. Treiman (2000). A site-conditions map for California based on geology and shear-wave velocity, *Bull. Seism. Soc. Am.* **90,** S187–S208.

Youd, T. L., J. P. Bardet, and J. D. Bray (Editors) (2000). Kocaeli, Turkey, earthquake of August 17, 1999, reconnaissance report, *Earthquake Spectra* **16** (Suppl. A), 65–96.

Zeng, Y., and C. H. Chen (2001). Fault rupture process of the 20 September 1999 Chi-Chi, Taiwan, earthquake, *Bull. Seism. Soc. Am.* **91,** 1088–1098.

ABS Consulting, Inc, and EQECAT, Inc.
1030 NW 161st Place
Beaverton, Oregon 97006
(K.W.C.)

Applied Technology & Science
5 Third Street, Suite 622
San Francisco, California 94103
(Y.B.)

Manuscript received 18 January 2002.